

Quantum information scrambling in adiabatically-driven critical systems

Ricardo Puebla^{1,†}, Fernando J. Gómez-Ruiz^{2,*}

¹*Departamento de Física, Universidad Carlos III de Madrid, Avda. de la Universidad 30, 28911 Leganés, Spain*

²*Departamento de Física Teórica, Atómica y Óptica, Universidad de Valladolid, 47011 Valladolid, Spain*

Correspondence: †rpuebla@fis.uc3m.es and *fernandojavier.gomez@uva.es

Abstract

Quantum information scrambling refers to the spread of the initially stored information over many degrees of freedom of a quantum many-body system. Information scrambling is intimately linked to the thermalization of isolated quantum many-body systems and has been typically studied in a sudden quench scenario. Here we extend the notion of quantum information scrambling to critical quantum many-body systems undergoing an adiabatic evolution. In particular, we analyze how the symmetry-breaking information of an initial state is scrambled in adiabatically-driven integrable systems, such as the Lipkin-Meshkov-Glick and quantum Rabi model. Following a time-dependent protocol that drives the system from a symmetry-breaking to a normal phase, we show how the initial information is scrambled even for perfect adiabatic evolutions as indicated by the expectation value of a suitable observable. We detail the underlying mechanism for quantum information scrambling, its relation to ground- and excited-state quantum phase transitions and quantify the degree of scrambling in terms of the number of eigenstates that participate in the encoding of the initial symmetry-breaking information. While the energy of the final state remains unaltered in an adiabatic protocol, the relative phases among eigenstates are scrambled and so is the symmetry-breaking information. We show that a potential information retrieval, following a time-reversed protocol, is hindered by small perturbations as indicated by a vanishingly small Loschmidt echo and out-of-time-ordered correlators. The reported phenomenon is amenable for its experimental verification and may help in the understanding of information scrambling in critical quantum many-body systems.

Keywords: Nonequilibrium critical dynamics, quantum phase transitions, quantum information scrambling

1 Introduction

The process by which quantum information, initially localized within the degrees of freedom of a many-body system, propagates and becomes distributed across the entire system degrees of freedom is known as information scrambling [1, 2, 3]. This phenomenon is particularly intriguing from a fundamental perspective, as it delves into the mechanisms of information dispersal and entanglement in complex quantum systems [4, 5, 6]. Understanding how this scrambling occurs can shed light on the underlying principles governing quantum dynamics and may have significant implications in quantum computing [7], quantum chaos [8], quantum thermodynamics [9, 10, 11, 6], and high energy physics [12].

Quantum many-body systems offer an unrivaled testbed platform to explore the rich interplay between entanglement, thermalization, non-equilibrium dynamics, and even quantum phase transitions (QPTs) [13, 14, 15]. Quantum information scrambling has been primarily linked with thermalization in closed systems, and thus it is intimately related to chaotic behavior in quantum many-body systems [13, 16, 17, 18, 9, 19, 20, 21]. The complex nature of correlations in non-integrable systems reveals itself in signatures of information scrambling [22], typically measured in terms of out-of-time-ordered correlation (OTOCs) functions and the Loschmidt echo [1, 2, 3]. Such scrambling of information has been extensively studied in a sudden-quench scenario [23, 24, 25, 26, 19, 20, 27, 28], where an initial state evolves under its governing and constant Hamiltonian. The integrability of the system has a profound impact on how the information gets scrambled, being non-integrable systems better scramblers as evidenced by the dynamics of OTOCs and Loschmidt echo (see for example [26]). The role of time-dependent quenches in quantum information scrambling remains, however, largely unexplored, and more so when involving critical features of a quantum many-body system.

In this work, we aim at closing this gap and analyze quantum information scrambling in critical systems undergoing a fully coherent adiabatic protocol. The considered systems feature a normal and symmetry-breaking phase where a \mathbb{Z}_2 parity is spontaneously broken. The initial information consists in one of the two possible symmetry-breaking choices and is encoded in an initial state that populates a large collection of degenerate energy eigenstates that break the discrete parity symmetry of the governing Hamiltonian. Such symmetry-breaking information remains unaltered under the dynamics of the initial Hamiltonian. This is possible for systems where a symmetry-breaking phase is not only restricted to the ground and first excited states, but rather it propagates up to a certain critical excitation energy [29, 30, 31, 32, 33, 34, 35, 36, 37, 38, 39, 40, 41, 42]. This is indeed the case for many-body systems with few effective and collective degrees of freedom, such as the Lipkin-Meshkov-Glick (LMG) model [43, 44, 45, 46, 47, 48], Dicke model [49, 50] or quantum Rabi model (QRM) [51, 52, 53, 54, 55]. These systems feature a ground-state mean-field quantum phase transition, as well as an excited-state quantum phase transition precisely at a critical excitation energy that divides the spectrum between normal (energy eigenstates with well-defined parity) and a degenerate phase, where eigenstates with opposite parities are degenerated by pairs, as described by a standard double-well semiclassical potential. We stress that the LMG and the QRM are integrable systems, while the Dicke model exhibits a region with chaotic behavior at sufficiently high excitation energies [56, 57, 58, 59]. It is worth remarking that the paradigmatic one-dimensional Ising model with a transverse field does not meet the previous criterion since only the two lowest energy eigenstates are degenerate in the antiferro- or ferromagnetic phase separated by the quantum phase transition [15].

The adiabatic protocol brings the initial symmetry-breaking state towards the normal and back to the degenerate phase by quenching the control parameter of the system. Albeit the populations of the energy eigenstates remain constant under the adiabatic theorem, the symmetry-breaking information is scrambled due to the different and non-commensurable relative phases gained during the protocol, provided the system is driven into the normal phase. Such dynamical phases are uniformly distributed resulting in an *adiabatic quantum information scrambling* (AQIS). The effectiveness of AQIS is illustrated in the LMG model, and quantified in terms of the final expectation value of a suitable symmetry-breaking observable, the number of populated eigenstates, as well as with the OTOCs. The robustness of the AQIS is analyzed by means of the Loschmidt echo between an

adiabatically evolved state, and its time-reversed protocol with a small perturbation. The AQIS is illustrated for different initial states and another integrable quantum critical model, namely, the QRM [51].

The article is organized as follows. In Sec. 2 we present the mechanism that leads to the quantum scrambling of symmetry-breaking information for an adiabatically-driven quantum many-body system, i.e. the AQIS. In Sec. 3 we first introduce the LMG model and then present numerical results of the adiabatic quantum information scrambling. A different model, the QRM, is analyzed in Sec. 4 and presents similar numerical results supporting the quantum information scrambling. Finally, in Sec. 5 we summarize the main results of the article.

2 Adiabatic Quantum Information Scrambling

Let us start considering a quantum critical system described by a Hamiltonian $\hat{H}(g)$ that depends on an external controllable parameter g , such that

$$\hat{H}(g) = \sum_{k=0} E_k(g) |\phi_k(g)\rangle \langle \phi_k(g)|, \quad (1)$$

where $E_k(g)$ denote the energy of the k th eigenstate $|\phi_k(g)\rangle$ for g . In addition, we assume that the Hamiltonian commutes with a discrete parity operator $\hat{\Pi}$, $[\hat{H}(g), \hat{\Pi}] = 0$ so that the eigenstates can be labeled in terms of the eigenvalues of $\hat{\Pi}$, $+1$ or -1 , owing to a \mathbb{Z}_2 symmetry, i.e. the eigenstates can be written as $|\phi_{k,\pm}(g)\rangle$ with $\hat{\Pi}|\phi_{k,\pm}(g)\rangle = \pm 1|\phi_{k,\pm}(g)\rangle$, and similarly for its energy $E_{k,\pm}(g)$, so that

$$\hat{H}(g) = \sum_{\substack{k=0 \\ p=\pm}} E_{k,p}(g) |\phi_{k,p}(g)\rangle \langle \phi_{k,p}(g)|. \quad (2)$$

The phase diagram of the Hamiltonian can be split in two regions, namely, normal phase where $E_{k,+}(g) \neq E_{k,-}(g)$ and a symmetry-breaking phase where the eigenstates belonging to a different parity subspace are degenerate, i.e. $E_{k,+}(g) = E_{k,-}(g)$, possibly up to a certain critical excitation energy $E_c(g)$. These two phases are separated by ground- and excited-state quantum phase transition [15, 29, 30, 31, 32, 33, 34, 35, 36, 37, 38], taking place a critical value g_c and at an excitation energy $E_c(g)$, respectively. Note that in the symmetry-breaking phase, any state of the form $|\phi(g)\rangle = \alpha|\phi_{k,+}(g)\rangle + \beta|\phi_{k,-}(g)\rangle$ with $|\alpha|^2 + |\beta|^2 = 1$ and $E_{k,+}(g) = E_{k,-}(g)$ is also a valid eigenstate of $\hat{H}(g)$. Yet, for any α such that $|\alpha| \neq 1, 0$, $|\phi(g)\rangle$ is no longer an eigenstate of the parity operator, $\hat{\Pi}|\phi(g)\rangle \neq \pm|\phi(g)\rangle$, and thus the symmetry may be spontaneously broken. This effect can be quantified employing the expectation value of a suitable operator $\hat{\mathcal{O}}$, such that $\langle \phi_{k,+}(g_0)|\hat{\mathcal{O}}|\phi_{k,-}(g_0)\rangle \neq 0$ and $\langle \phi_{k,p}(g_0)|\hat{\mathcal{O}}|\phi_{k,p}(g_0)\rangle = 0$. Indeed, its expectation value behaves as an order parameter, i.e. $\langle \hat{\mathcal{O}} \rangle = 0$ for a symmetric state and $\langle \hat{\mathcal{O}} \rangle \neq 0$ for symmetry-breaking states, as it is the case for the magnetization in a standard ferro-to-paramagnetic phase transition.

We consider an initial state $|\psi_0\rangle$ which breaks this symmetry for an initial value g_0 of the control parameter in the symmetry-breaking phase, i.e. $\langle \psi_0|\hat{\mathcal{O}}|\psi_0\rangle \neq 0$. This is the information we will consider throughout the rest of the article. Note that in general $[\hat{H}(g), \hat{\mathcal{O}}] \neq 0$. Such state can be written in the eigenbasis of $\hat{H}(g_0)$ as

$$|\psi_0\rangle = \sum_{\substack{k=0 \\ p=\pm}} c_{k,p} |\phi_{k,p}(g_0)\rangle. \quad (3)$$

The coefficients $c_{k,p}$ encode therefore the choice of the symmetry-breaking state, and thus the initial information. Moreover, since $\hat{O} = \sum_n \gamma_n |\gamma_n\rangle \langle \gamma_n|$, we can characterize the probability distribution of measuring γ_n 's in the initial state $|\psi_0\rangle$, which reads as

$$P(\gamma_n) = |\langle \psi_0 | \gamma_n \rangle|^2 = \left| \sum_{k,p=\pm} c_{k,p}^* \langle \phi_{k,p}(g_0) | \gamma_n \rangle \right|^2. \quad (4)$$

For a symmetric state, $P(\gamma_n) = P(-\gamma_n)$ and thus $\langle \hat{O} \rangle = 0$. However, for maximally symmetry-broken states, the distribution is only non-zero for one of the two branches, i.e. either $P(\gamma > 0) \neq 0$ or $P(\gamma < 0) \neq 0$. For simplicity, and without loss of generality, we will consider initial maximally symmetry-broken states $|\psi_0\rangle$ where $P(\gamma > 0) \neq 0$ and $P(\gamma < 0) = 0$. In addition, note that the energy probability distribution of the initial state is simply given by $P(E_k(g)) = |c_{k,+}|^2 + |c_{k,-}|^2$, since we consider the initial state to be in the symmetry-breaking phase. Therefore, $P(E)$ is independent of the initial information, and thus the energy probability distribution does not depend on how the symmetry is broken.

We then consider a time-dependent protocol $g(t)$ that drives the system from $g(0) = g_0$ to $g(\tau) = g_1$, and back to the initial control value, $g(2\tau) = g_0$. For simplicity, we consider a linear ramp, namely,

$$g(t) = \begin{cases} g_0 + (g_1 - g_0) \frac{t}{\tau}, & \text{for } 0 \leq t \leq \tau, \\ g_1 + (g_0 - g_1) \frac{(t-\tau)}{\tau}, & \text{for } \tau \leq t \leq 2\tau. \end{cases} \quad (5)$$

We also assume that the driving is performed very slowly, allowing us to resort to the adiabatic approximation for the final state, $|\psi(2\tau)\rangle$. Indeed, one can write

$$|\psi(2\tau)\rangle \approx \sum_{k,p} c_{k,p} e^{-i\varphi_{k,p}} |\phi_{k,p}(g_0)\rangle, \quad (6)$$

where $\varphi_{k,p}$ denotes the accumulated phase for the k -th eigenstate of parity p upon completing the cycle from g_0 to g_1 and back to g_0 , i.e.

$$\varphi_{k,p} = \frac{2\tau}{(g_1 - g_0)} \int_{g_0}^{g_1} dg E_{k,p}(g). \quad (7)$$

Under the adiabatic approximation, neither the average energy nor the energy probability distribution $P(E)$ are altered. The relative phases between degenerate eigenstates are irrelevant to the energy, as commented above. However, the symmetry-breaking information may be largely affected since $\langle \phi_{k,+}(g_0) | \hat{O} | \phi_{k,-}(g_0) \rangle \neq 0$, and thus $\langle \psi(2\tau) | \hat{O} | \psi(2\tau) \rangle$ will depend on the phases $\varphi_{k,p}$, and will be, in general, different from the initial condition $\langle \psi(2\tau) | \hat{O} | \psi(2\tau) \rangle \neq \langle \psi_0 | \hat{O} | \psi_0 \rangle$.

We can explicitly write the expression for the expectation value of \hat{O} after the completion of the cycle. Assuming that $\langle \phi_{k,p}(g_0) | \hat{O} | \phi_{k,p}(g_0) \rangle = 0$ for $p = +, -$, then

$$\langle \psi(2\tau) | \hat{O} | \psi(2\tau) \rangle = \sum_{k,k'} c_{k,+} c_{k',-}^* e^{-i(\varphi_{k,+} - \varphi_{k',-})} \langle \phi_{k',-}(g_0) | \hat{O} | \phi_{k,+}(g_0) \rangle + \text{H.c.} \quad (8)$$

Now, since only the eigenstates with the same k label and opposite parity are degenerate, then we can further simplify the previous expression and find

$$\langle \psi(2\tau) | \hat{O} | \psi(2\tau) \rangle \approx \sum_k c_{k,+} c_{k,-}^* e^{-i(\varphi_{k,+} - \varphi_{k,-})} \langle \phi_{k,-}(g_0) | \hat{O} | \phi_{k,+}(g_0) \rangle + \text{H.c.} \quad (9)$$

If the initial state populates just a single doublet, e.g. only the coefficients $c_{0,+}$ and $c_{0,-}$ are non-zero, then the final value will be present an oscillatory behavior $\langle \psi(2\tau) | \hat{O} | \psi(2\tau) \rangle \propto \cos[\delta\varphi_0] \langle \psi_0 | \hat{O} | \psi_0 \rangle$, where $\delta\varphi_0 = \varphi_{0,+} - \varphi_{0,-} = 2\tau/(g_1 - g_0) \int_{g_0}^{g_1} dg (E_{k,+}(g) - E_{k,-}(g))$ is the difference between the phases, depending on τ . In this manner, tuning τ (assuming that the adiabatic approximation holds), the symmetry breaking observable can be in any value between $\langle \psi_0 | \hat{O} | \psi_0 \rangle$ and $-\langle \psi_0 | \hat{O} | \psi_0 \rangle$. Hence, the information regarding the initial symmetry breaking is not scrambled, as the expectation value $\langle \psi(2\tau) | \hat{O} | \psi(2\tau) \rangle$ may reverse or not the initial value by simply tuning τ . Yet, when the initial state populates a large number of eigenstates, and if the difference in the accumulated phases $\delta\varphi_k$ for different k 's uniformly sample the interval $[0, 2\pi)$, then,

$$\langle \psi(2\tau) | \hat{O} | \psi(2\tau) \rangle \approx 0, \quad (10)$$

regardless of the specific time τ . Note that the phase differences $\delta\varphi_k$ will only be non-zero if the system is driven from the symmetry-breaking to the normal phase, as otherwise $E_{k,+} = E_{k,-}$ leading to $\delta\varphi_k = 0$. Hence, the mechanism for AQIS requires g_0 to be in the symmetry-breaking and g_1 in the normal phase, thus forcing the system to traverse the excited-state quantum phase transition.

A consequence of Eq. (10) is that the probability distribution of the operator \hat{O} for the final state $|\psi(2\tau)\rangle$ will exhibit a balanced distribution for $\gamma < 0$ and $\gamma > 0$, as it were a symmetric state. In this manner, the initial symmetry-breaking information is scrambled in the quantum system due to the large number of populated eigenstates. We can anticipate that the expression given in Eq. (10), i.e. AQIS will be more effective the larger the support of the initial state over the eigenstates of $\hat{H}(g_0)$. In the following, we illustrate the AQIS in the LMG and QRM models, supporting with numerical simulations its effectiveness, robustness, and dependence on different initial states.

3 Lipkin-Meshkov-Glick model

The LMG model [43], originally introduced in the context of nuclear physics, describes the long-range dipole-dipole interaction of N spin- $\frac{1}{2}$ under a transverse magnetic field. This model exhibits a QPT [15] at a certain critical value of the field strength g_c [44, 45, 46, 47, 48], and has attracted renewed attention due to its experimental realization, e.g. with cold atoms [60] or in trapped ions [61]. Indeed, the LMG has served as a test bed for the exploration of different aspects of quantum critical systems [62, 63, 64, 65, 66, 67, 37, 68, 69, 70, 71, 72, 73, 74, 75, 39, 76]. The Hamiltonian of the N spin- $\frac{1}{2}$ particles can be written as (unit of frequency equal to 1, and $\hbar = 1$)

$$\hat{H}_{\text{LMG}} = -g\hat{S}_z - \frac{\hat{S}_x^2}{N}, \quad (11)$$

where $\hat{S}_\alpha = \sum_{k=1}^N \hat{\sigma}_\alpha/2$ are the collective spin-1/2 operators along α -direction ($\alpha = x, y, z$). Since the $\hat{H}(g)$ commutes with $\hat{S}^2 = \hat{S}_x^2 + \hat{S}_y^2 + \hat{S}_z^2$, we restrict ourselves to the sector of maximum spin, i.e. $J = N/2$, and work in the Dicke basis, $\hat{S}_z |J, M\rangle = M |J, M\rangle$ with $-J \leq M \leq J$, and $\hat{S}^2 |J, M\rangle = J(J+1) |J, M\rangle$. For simplicity, we will consider N even. In the $N \rightarrow \infty$, the previous Hamiltonian features a QPT at the critical value $g_c = 1$ [48, 47], which divides the spectrum into two phases (see Fig. 1 for a representation of the energy spectrum for $N = 300$ spins). For $g < g_c$, there is a symmetry-breaking \mathbb{Z}_2 phase up to critical energy $E_c(g)$ dependent on g where the eigenstates of different parity are degenerate; to the contrary, for energies above $E_c(g)$ or for $g > g_c$, there

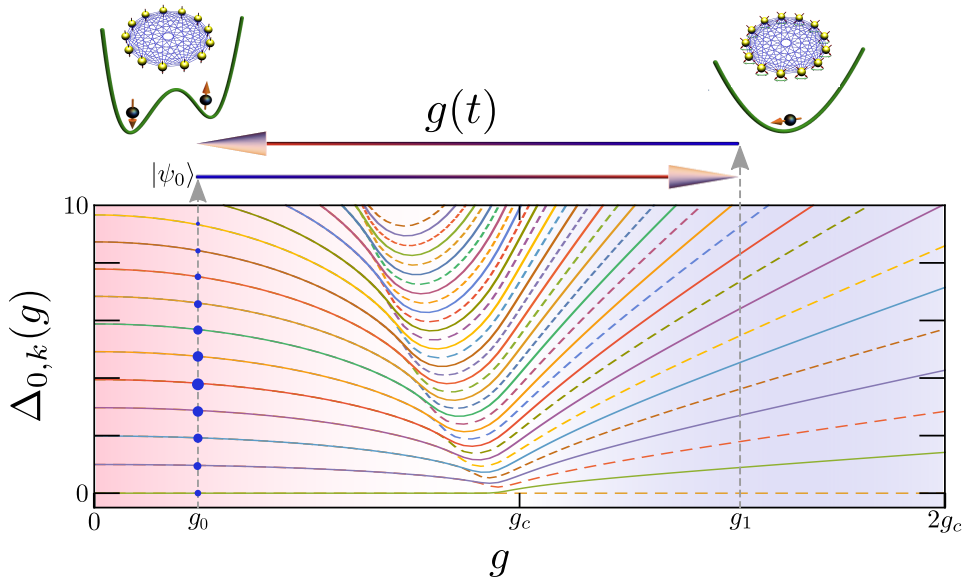


Figure 1: **Sketch of protocol that leads to an adiabatic scrambling of information.** Information is encoded in an initially symmetry-breaking state $|\psi_0\rangle$, which populates a large collection of eigenstates in the symmetry-broken phase of the model at $g_0 < g_c$. The system then undergoes a coherent adiabatic cycle $g(t)$ entering into the normal phase and back. The populations of the initial state remain unaltered, while the information is scrambled due to the change in the relative phases among degenerate eigenstates. The energy spectrum corresponds to the LMG for $N = 300$ spins, where $\Delta_{0,k}(g) = E_k(g) - E_0(g)$ with dashed- and solid-lines depicting the energies of even and odd parity eigenstates, respectively.

is a normal phase where the parity is well defined and the eigenstates are no longer degenerate. The location of the critical excitation energy $E_c(g)$ corresponds to the so-called excited-state quantum phase transition (ESQPT), whose main hallmark consists in a logarithmically-diverging density of states at $E_c(g)$ [45, 36, 29, 77, 30, 31, 52, 78, 32, 33]. In the LMG model, the spin operator \hat{S}_x plays the role of the operator \hat{O} introduced in Sec. 2, whose ground-state expectation value serves as a good order parameter for the ground-state QPT.

In the following, we illustrate how the mechanism described in Sec. 2 applies to the LMG model, i.e. the adiabatic quantum information scrambling of the symmetry-breaking initial state. To study the effectiveness of AQIS as a function of the number of populated eigenstates, i.e. the validity of Eq. (10), we first consider an initial microcanonical-like state that uniformly populates the first $2N_{\text{mc}}$ eigenstates. That is,

$$|\psi_0\rangle = \frac{1}{\sqrt{2N_{\text{mc}}}} \sum_{k=0}^{N_{\text{mc}}-1} (|\phi_{k,+}(g_0)\rangle + x_k |\phi_{k,-}(g_0)\rangle), \quad (12)$$

where the coefficients $x_k = -1, +1$ are chosen according to the sign of $\langle \phi_{k,+} | \hat{S}_x | \phi_{k,-} \rangle$ so that $\langle \psi_0 | \hat{S}_x | \psi_0 \rangle$ is positive, and the probability distribution $P(S_x)$ only shows non-zero values in the positive branch. See Fig. 2(a) and (b) for the initial probability distribution of this microcanonical-

like state where $g_0 = 0$, $N = 100$ spins with $N_{\text{mc}} = 10$. The dynamical protocol follows Eq. (5) with $g_1 = 1.25$ to ensure that the system is completely driven into the normal phase (cf. Fig. 1). The final probability distributions are also plotted in Fig. 2(a) and (b), for the \hat{S}_x and energy, respectively. Considering slow ramps ($\tau \gg 1$) we first note that the energy probability distribution $P(E)$ remains unaltered, i.e. the coefficients $c_{k,p}$ approximately hold constant. To the contrary, $P(S_x)$ significantly differs from the initial distribution as a consequence of the AQIS. The final state $|\psi(2\tau)\rangle$ populates both branches of the observable \hat{S}_x , and thus its expectation value after the completion of the cycle vanishes, $\langle\psi(2\tau)|\hat{S}_x|\psi(2\tau)\rangle \approx 0$. This can be better visualized in Fig. 2(c) where we show the evolution of $\langle\psi(t)|\hat{S}_x|\psi(t)\rangle$ as a function of $g(t)$. Since the dynamical evolution is to a very good approximation adiabatic, other observables not related to the symmetry-breaking information remain unchanged, such as \hat{S}_z or the energy (cf. Fig. 2(d)). In the following, and to ease the numerical simulations, we assume that the evolution is adiabatic and thus make use of the approximation given in Eq. (6) to compute the final state after the cycle.

3.1 Effectiveness of the quantum information scrambling

The effectiveness of the AQIS of the symmetry-breaking information is intimately related to the distribution of the phases $\delta\varphi_k$, i.e. the difference of the accumulated phase among eigenstates of opposite parity, as discussed in Sec. 2. Thus, the proper quantum information scrambling requires $\delta\varphi_k$ to uniformly sample $[0, 2\pi)$. In Fig. 3 we show the resulting distribution of these phases $\delta\varphi_k$ for a LMG model comprising $N = 2000$ spins and for the first 200 eigenstates and $\tau = 10^3$ with $g_0 = 0$ and $g_1 = 1.25$. Note that it approximately corresponds to a uniform distribution in the range $[0, 2\pi)$. Similar results can be found for other choices of τ , N , g_0 , and g_1 , provided g_1 ensures that the system enters in the normal phase. Otherwise, i.e. if the system remains in the symmetry-breaking phase during the whole cycle, then $\delta\varphi_k = 0 \forall k$ since $E_{k,+}(g) = E_{k,-}(g)$ during the protocol and the information scrambling will not occur.

As commented in Sec. 2, the effectiveness of AQIS depends on the number of populated eigenstates in the initial state, i.e. on the support of $|\psi_0\rangle$ on the eigenstates of $\hat{H}(g_0)$. The initial state given in Eq. (12) allows us to systematically analyze the validity of Eq. (10) as N_{mc} increases. We first note that, if $N_{\text{mc}} \approx 1$ the final expectation value of \hat{S}_x will simply undergo an oscillatory dependent on τ . This can be seen in Fig. 4(a) for an initial state with $N_{\text{mc}} = 4$, which hardly scrambles the symmetry-breaking information as one can recover the initial value $\langle\psi_0|\hat{S}_x|\psi_0\rangle$ at a suitable time τ . Yet, as N_{mc} grows, this is no longer the case due to the uniform distribution of the phases $\delta\varphi_k$, which forces the final expectation value to average to zero, i.e. $\langle\psi(2\tau)|\hat{S}_x|\psi(2\tau)\rangle \approx 0$. The effectiveness of AQIS can be therefore quantified in terms of the fluctuations of $\langle\psi(2\tau)|\hat{S}_x|\psi(2\tau)\rangle$ around its average value, i.e.

$$\sigma^2(S_x) = \overline{\left(\langle\psi(2\tau)|\hat{S}_x|\psi(2\tau)\rangle - \overline{\langle\psi(2\tau)|\hat{S}_x|\psi(2\tau)\rangle}\right)^2}. \quad (13)$$

In the previous expression \overline{X} corresponds to the average value of X in an interval of quench times $\tau \in [\tau_0, \tau_1]$, where τ_0 already ensures the validity of the adiabatic approximation. If the information is perfectly scrambled, then $\sigma^2(S_x) = 0$ so that the adiabatically-evolved final state features $\langle\psi(2\tau)|\hat{S}_x|\psi(2\tau)\rangle = 0$ independently of τ . Therefore, the smaller $\sigma(S_x)$ the more effective is the AQIS. The results are plotted in Fig. 4(b) obtained for $\tau_0 = 10^3$ and $\tau_1 = 10^4$, and similar parameters as in previous figures, namely, $g_0 = 0$, $g_1 = 1.25$ and for two system sizes, $N = 1000$ and 2000 spins. As the number of populated states grows, N_{mc} , the variance $\sigma^2(S_x)$ decreases, thus

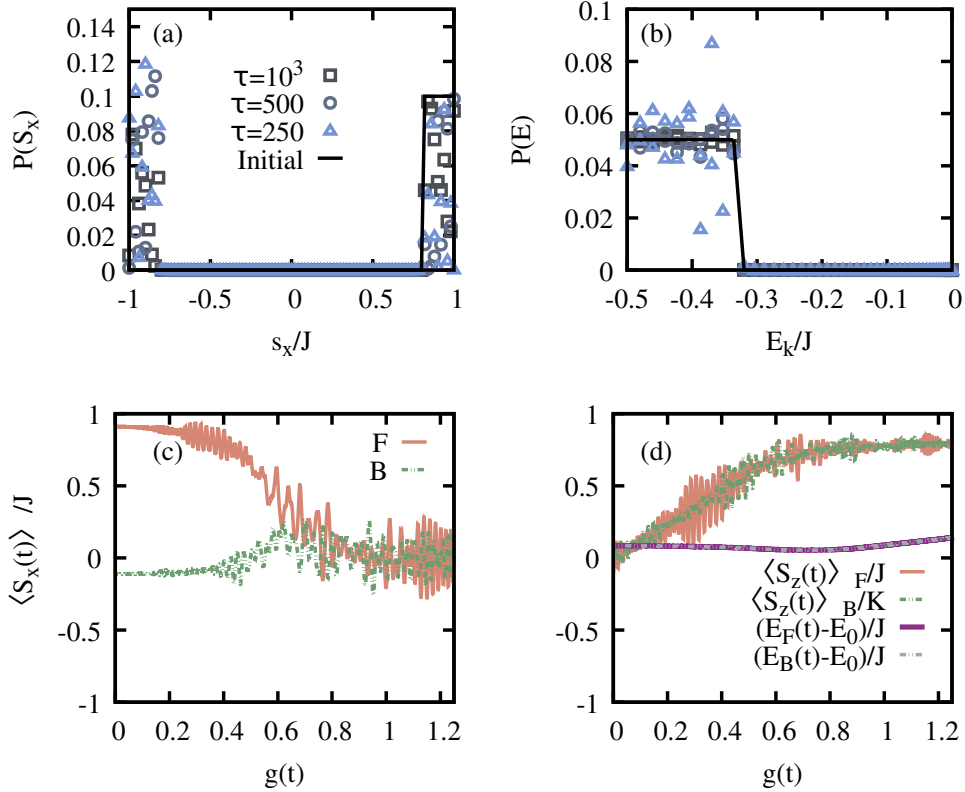


Figure 2: **Adiabatic quantum scrambling of the symmetry-breaking information in the LMG model.** Panel (a) shows the initial and final probability distribution over the observable \hat{S}_x for an initial microcanonical-like state undergoing a fully-coherent cycle from the symmetry-breaking to the normal phase and back. Panel (b) shows the energy probability distribution $P(E)$ for the initial and final states after the cycle (same τ values as in (a)). Panel (c) illustrates the dynamics of the expectation value $\langle \psi(t) | \hat{S}_x | \psi(t) \rangle$ as a function of the time-dependent control $g(t)$ for $\tau = 500$. Here F (B) denotes the forward (backward) process from $g_0 \rightarrow g_1$ ($g_1 \rightarrow g_0$). Note that $\langle S_x \rangle \approx 0$ after the adiabatic protocol. In (d) the dynamics of other relevant observables not related to the symmetry-breaking information are shown, and thus not scrambled during the adiabatic protocol. The employed parameters are $N = 100$ spins, $g_0 = 0$, $g_1 = 1.25$, $N_{\text{mc}} = 10$.

indicating a better-scrambling performance. A fit to the numerical results reveals a dependence $\sigma(S_x) \propto N_{\text{mc}}^{-2/3}$ (cf. Fig. 4(b)).

3.2 Loschmidt echo and out-of-time-ordered correlator

The previous results support the effectiveness of the AQIS of the symmetry-breaking information of the initial state $|\psi_0\rangle$. However, since the state evolves in a fully coherent manner, $|\psi(2\tau)\rangle = \hat{U}(2\tau)|\psi_0\rangle$ where $\hat{U}(t) = \hat{\mathcal{T}}e^{-i\int_0^t dt' \hat{H}(t')}$ corresponds to unitary time-evolution operator from 0 to t under the protocol $g(t)$, the initial state can be recovered by a perfect time-reversal operation, i.e. $|\psi_0\rangle = \hat{U}(2\tau)^\dagger |\psi(2\tau)\rangle$. This corresponds to an evolution of the final state under $\hat{H}(g) \rightarrow -\hat{H}(g) \forall g$. If such a time-reversal operation is perfect, then the symmetry-breaking information can be recovered from the scrambled state $|\psi(2\tau)\rangle$. However, as customary in closed systems,

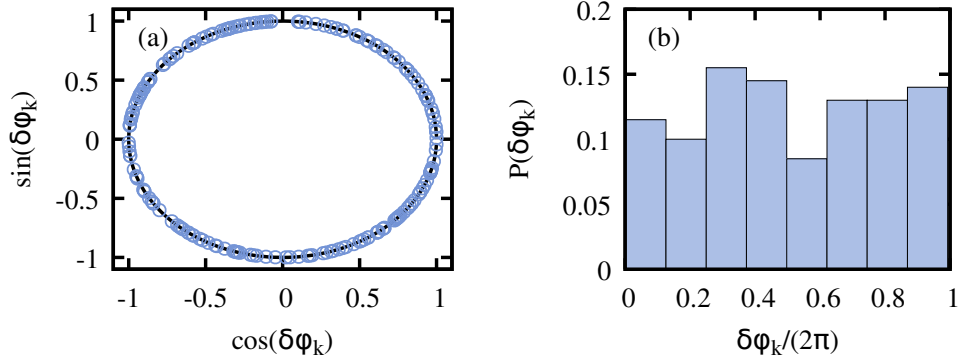


Figure 3: **Distribution of the phases $\delta\varphi_k$.** Panel (a) shows the obtained phases plotted in a unit circle, while the distribution of the phases in the range $[0, 2\pi)$ is shown in (b), revealing an approximately uniform distribution. The results correspond to the LMG model with $N = 2000$ spins and for the first 200 eigenstates, $\tau = 10^3$ with $g_0 = 0$ and $g_1 = 1.25$.

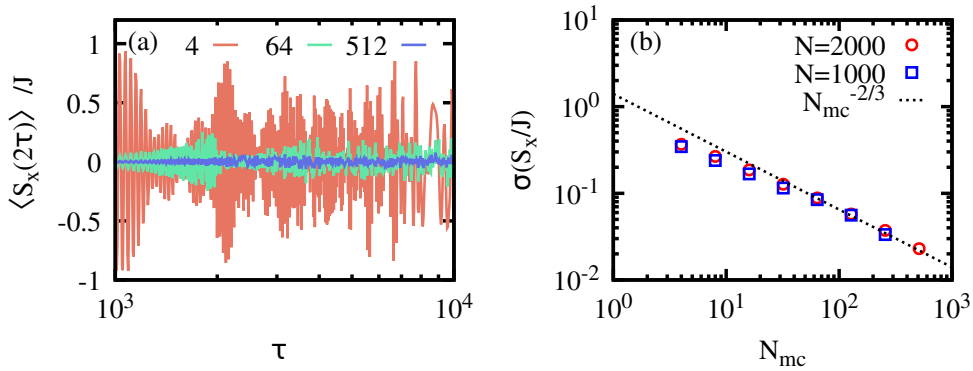


Figure 4: **Effectiveness of the AQIS as a function of the number of populated eigenstates.** Panel (a) shows the final expectation value of \hat{S}_x , i.e. $\langle\psi(2\tau)|\hat{S}_x|\psi(2\tau)\rangle$ as a function of τ , ensuring the adiabatic approximation, and for a different number of populated eigenstates N_{mc} , i.e. 4, 64 and 512. Panel (b) shows the the resulting standard deviation of the results in (a) for their average value, as a function of N_{mc} . See the main text for further details.

the retrieval of the initial information highly depends on any potential deviation from a perfect time-reversal evolution, and thus any small mismatch will hinder the recovery of the initial state. This motivates the analysis of the Loschmidt echo,

$$L(\tau, \delta t) = |\langle\psi_0|\hat{U}^\dagger(2\tau + \delta t)\hat{U}(2\tau)|\psi_0\rangle|, \quad (14)$$

which quantifies the overlap between the final state $|\psi(2\tau)\rangle = \hat{U}(2\tau)|\psi_0\rangle$ and the potentially restored initial state upon a time-reversal evolution with a small time-delay δt . Hence, for $\delta t = 0$ it follows $L(\tau, \delta t = 0) = 1 \forall \tau$. The scrambling due to AQIS will be robust the smaller the Loschmidt echo for small time-delays, i.e. if $L(\tau, \delta t) \approx 0$ for $\delta t \ll 1$.

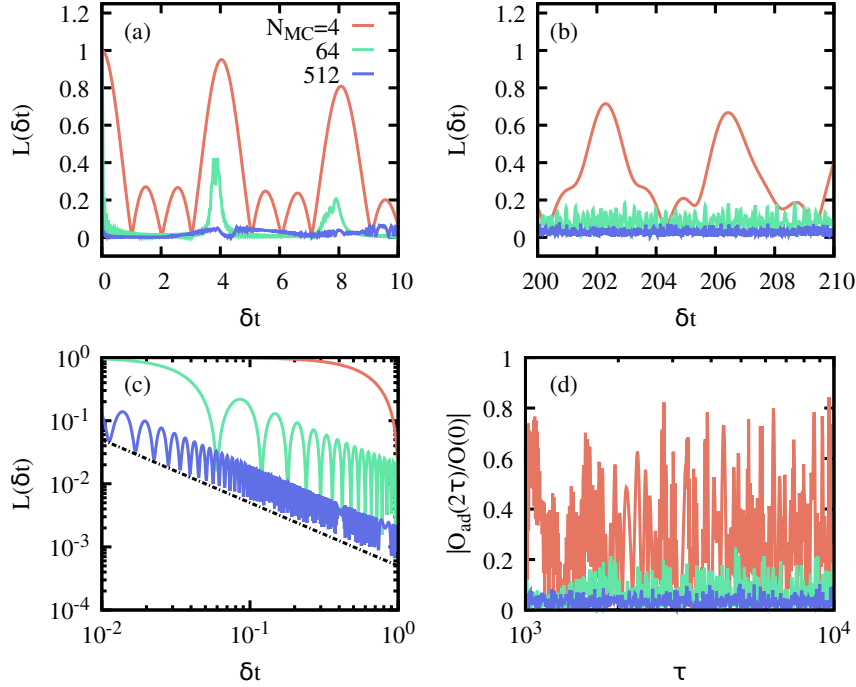


Figure 5: **Loschmidt echo and OTOC for the LMG model.** Panels (a), (b), and (c) show the Loschmidt echo $L(\delta t)$ as a function of the time mismatch δt and for initial states with different populated eigenstates N_{mc} . Note that strong revivals even at late times (b), and the decaying echo $1/\delta t$ (dashed line) in (c) when $N_{\text{mc}} \gg 1$. Panel (d) corresponds to a rescaled OTOC which signals a similar behavior to the expectation value of S_x . The simulation parameters are $N = 2000$ spins, $g_0 = 0$ and $g_1 = 1.25$. See the main text for further details.

As we are interested in an adiabatic evolution, i.e. for sufficiently long τ , we rely again on the adiabatic approximation. It is easy to see that under this approximation one obtains the simple expression

$$L(\tau, \delta t) = \left| \sum_{\substack{k=0 \\ p=\pm}} |c_{k,p}|^2 e^{i\delta t \varphi_{k,p}} \right|, \quad (15)$$

with $\sum_{k,p} |c_{k,p}|^2 = 1$. Note that under the adiabatic approximation, the previous quantity does not depend on τ , i.e. $L(\tau, \delta t) \equiv L(\delta t)$. Again, as for the effectiveness of AQIS (Eq. (10)), initial states with a large support and uniformly distributed phases $\varphi_{k,p}$, one expects $L(\delta t) \approx 0$ even for $0 < \delta t \ll 1$. The results are plotted in Fig. 5(a)-(c), which precisely reveal a vanishingly small echo $L(\delta t) \approx 0$ for small time mismatches δt . Although not explicitly shown, we note that similar results can be obtained if instead of a time mismatch δt a deviation in other quantity is considered, such as in $g_{0,1}$. In particular, we observe a decay $L(\delta t) \propto 1/\delta t$ for short δt and $N_{\text{mc}} \gg 1$. As expected, in states with small support (few populated eigenstates), $L(\delta t)$ displays large revivals and never decays to 0, a clear indication of the failure of quantum information scrambling.

As commented in Sec. 1, OTOCs have been proven a valuable tool for studying information scrambling. In a sudden quench scenario, scrambling is related to the short-time behavior of the OTOC

for a relevant observable [26]. In our case, we can define the OTOC as

$$\begin{aligned} O(t) &= \langle \psi_0 | \hat{S}_x(t) \hat{S}_x \hat{S}_x(t) \hat{S}_x | \psi_0 \rangle, \\ &= \langle \psi_0 | \hat{U}^\dagger(t) \hat{S}_x \hat{U}(t) \hat{S}_x \hat{U}^\dagger(t) \hat{S}_x \hat{U}(t) \hat{S}_x | \psi_0 \rangle. \end{aligned} \quad (16)$$

Since the AQIS is effective only after the cycle has been completed, we focus on $O(2\tau)$. Again, relying on the adiabatic approximation of the evolved state, we approximate $\hat{U}(2\tau)$ by its adiabatic counterpart $\hat{U}^{\text{Ad}}(2\tau)$, so the populations in the eigenbasis of the instantaneous Hamiltonian remain constant and the only change is due to the accumulated phase during the cycle. In this manner, we can compute the adiabatic OTOC, denoted here as $O^{\text{Ad}}(2\tau)$ and fulfilling $O^{\text{Ad}}(2\tau) \approx O(2\tau)$ for $\tau \gg 1$. The results for $O^{\text{Ad}}(2\tau)$, plotted in Fig. 5(d), reveal essentially the same behavior as $\langle \psi(2\tau) | \hat{S}_x | \psi(2\tau) \rangle$. That is, the adiabatic dynamics scramble the symmetry-breaking information contained in the initial state, and thus $O(2\tau) \approx 0$. This becomes more effective the more eigenstates are significantly populated in the initial state. Conversely, for small support (e.g. $N_{\text{mc}} = 4$ corresponding to the red line in Fig. 5(d)), the OTOC features large oscillations, potentially reaching its initial value.

3.3 Symmetry-breaking thermal states

Having systematically analyzed the mechanism of AQIS in the LMG model and its effectiveness in terms of the number of populated eigenstates, we turn now our attention to a different initial state. Moreover, we will study how the reported AQIS depends on the control parameter g_1 , i.e. on whether the system is driven from the symmetry-breaking into the normal phase or not.

Here, we consider a different initial state, namely, a symmetry-breaking thermal state with inverse temperature β ($k_b = 1$),

$$\hat{\rho}_{\beta,SB} = \frac{1}{Z} \sum_k e^{-\beta E_k(g_0)} |\psi_{k,SB}(g_0)\rangle \langle \psi_{k,SB}(g_0)|, \quad (17)$$

where Z is the partition function that ensures a proper normalization of the state, $\text{Tr}[\hat{\rho}_{\beta,SB}] = 1$, while $|\psi_{k,SB}(g_0)\rangle = \frac{1}{\sqrt{2}}(|\psi_{k,+}(g_0)\rangle + x_k |\psi_{k,-}(g_0)\rangle)$ being $x_k = \pm 1$ depending on the expectation value of \hat{S}_x . As for Eq. (12), we consider a maximally symmetry-breaking state with $\text{Tr}[\hat{\rho}_{\beta,SB} \hat{S}_x] > 0$ so that $P(S_x)$ shows only non-zero probability for positive eigenvalues of \hat{S}_x (cf. Fig. 6(a)), while $P(E)$ displays the standard exponentially decaying populations (cf. Fig. 6(b)). Hence, the state $\hat{\rho}_{\beta,SB}$ corresponds to a thermal state projected onto one of the two symmetry-breaking branches, i.e. to a generalized Gibbs state.

We then analyze how the realization of the adiabatic cycle scrambles the initial information, depending on the value of g_1 . As shown in Fig. 1, to ensure that the whole state is driven into the normal phase, $g_1 > 1$. For a final value $g_1 < 1$, only a fraction of excited states will enter the normal phase, thus rendering the AQIS ineffective as $\delta\varphi_k = 0$ for those eigenstates that remain within the symmetry-breaking phase. The results are plotted in Fig. 6. As for the initial state given in Eq. (12), the final distribution $P(S_x)$ largely differs from the initial one since both branches are populated, ensured by $g_1 = 1.25$. For other choices of g_1 , the final $P(S_x)$ may fail to be a balanced distribution. This is shown in Fig. 6(c) where the final expectation value $\langle \hat{S}_x(2\tau) \rangle = \text{Tr}[\hat{U}(2\tau) \hat{\rho}_{\beta,SB} \hat{U}^\dagger(2\tau) S_x]$ is plotted as a function of τ and for three different values of g_1 . For $g_1 = 0.1$ the system remains in the symmetry-breaking phase during the whole cycle, and thus $\delta\varphi_k = 0 \forall k$ resulting in the

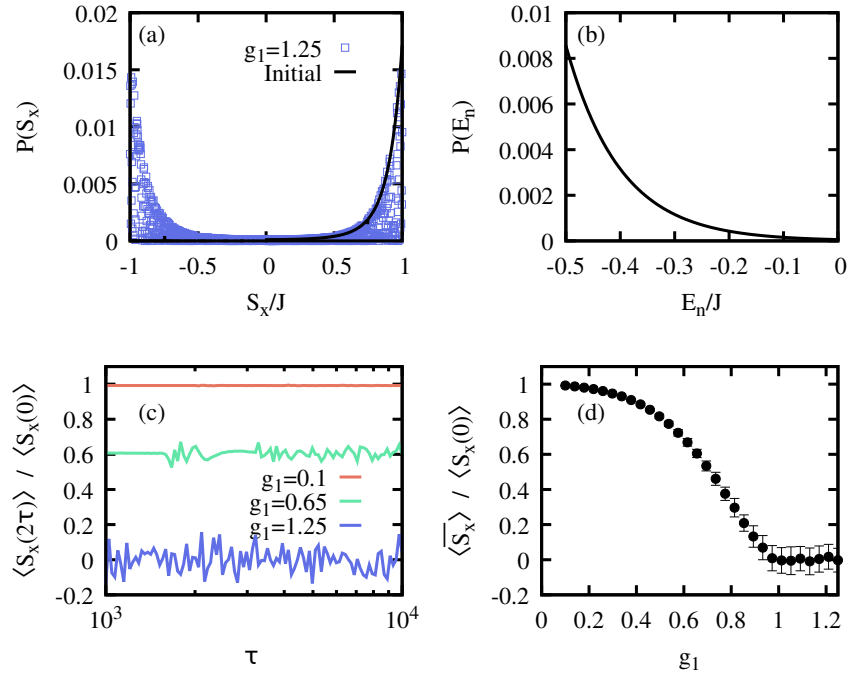


Figure 6: **AQIS for a symmetry-breaking thermal state in the LMG model.** (a) Initial probability distribution $P(S_x)$ over the observable \hat{S}_x for $\hat{\rho}_{\beta,SB}$ with $\beta = 0.02$ for $N = 10^3$ and $g_0 = 0$ (solid black line), together with the probability for the state upon an adiabatic protocol for $\tau = 10^3$ and $g_1 = 1.25$ (blue squares), which equally populates both S_x branches. (b) Population of the initial eigenstate for the symmetry-breaking thermal state $\hat{\rho}_{\beta,SB}$, as in (a). (c) Final expectation value of \hat{S}_x after an adiabatic protocol from $g_0 = 0$ to $g_1 = 0.1$ (red), 0.65 (green) and 1.25 (blue), as a function of τ and for $\hat{\rho}_{\beta,SB}$ with $\beta = 0.02$ and $N = 10^3$, as in (a) and (b). For $g_1 = 0.1$, the system is not driven into the normal phase. For $g = 0.65$, the state enters partially, while for $g_1 = 1.25$ it is driven completely into the normal phase, leading to a full AQIS. (d) Average expectation value of \hat{S}_x in the range $\tau \in \{10^3, 10^4\}$ as a function of the final coupling strength g_1 , revealing an order-parameter-like behavior. The error bars correspond to a standard deviation for the average of $\langle \hat{S}_x(2\tau) \rangle$. See main text for details.

absence of scrambling. For $g_1 = 0.65$, only a fraction of eigenstates are driven into the normal phase, partially scrambling the initial information. Finally, for $g_1 = 1.25$ the whole system enters in the normal phase, which corresponds to the AQIS discussed previously. To better visualize this effect, in Fig. 6(d) we show the average value of $\langle S_x(2\tau) \rangle$ in the range $\tau \in [10^3, 10^4]$ as a function of g_1 , which behaves as an order parameter for the AQIS.

4 Quantum Rabi model

The QRM describes the coherent interaction between a spin-1/2 and a single bosonic mode and thus constitutes a fundamental model in the realm of light-matter interaction and of key relevance

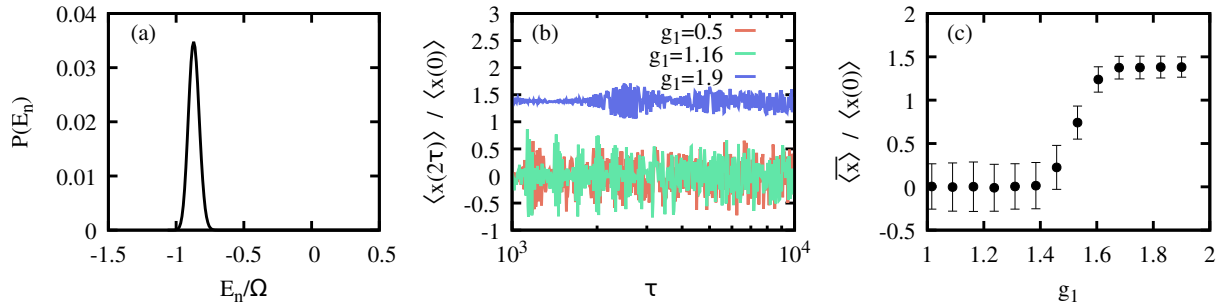


Figure 7: **AQIS for the QRM.** (a) Initial energy probability distribution $P(E_n)$ for $|\psi(0)\rangle = |\alpha\rangle_m |0\rangle_s$ for $\Omega = 100\omega$, initial rescaled coupling $g_0 = 2$ and $\alpha = 5$. The normal phase finds itself above the critical excitation energy $E_c/\Omega = -1/2$. Upon the adiabatic protocol, the energy probability distribution is equivalent to the initial one. (b) Expectation value of the symmetry-breaking observable \hat{x} after the adiabatic protocol of duration τ from $g_0 = 2$ to g_1 , as indicated in the key, assuming the adiabatic approximation. (c) Average symmetry-breaking expectation value, in the range $\tau \in \{10^3, 10^4\}$, as a function of the final coupling g_1 . For $g_1 \lesssim 1.5$, the whole state enters in the normal phase, leading into a complete adiabatic information scrambling. Error bars correspond to the standard deviation for $\langle \hat{x}(2\tau) \rangle$ as plotted in (b). See the main text for further details.

in quantum technologies. The Hamiltonian of the QRM can be written as

$$\hat{H}_{\text{QRM}}(\lambda) = \frac{\Omega}{2} \hat{\sigma}_z + \omega \hat{a}^\dagger \hat{a} + \lambda (\hat{a} + \hat{a}^\dagger) \hat{\sigma}_x, \quad (18)$$

where Ω , ω , and λ correspond to the frequency of the qubit, bosonic mode, and interaction strength among them. Despite comprising just a single spin, this model has been shown to display ground-, excited-state, and even dynamical quantum phase transitions in the limit of $\Omega/\omega \rightarrow \infty$ [53, 51, 52, 54]. In this particular parameter limit, which plays the role of the standard thermodynamic limit where critical phenomena typically take place, the ground-state QPT occurs at $\lambda_c = \sqrt{\omega\Omega}/2$. Hence, for convenience, we introduce the rescaled interaction strength, $g = \lambda/\lambda_c$ so that $g_c = 1$ as in the LMG.

The phase diagram of the critical QRM is divided into three regions. For $g < g_c$, a normal phase. For $g > g_c$, and energy $E_k(g) < E_c = -\Omega/2$, one finds the symmetry-breaking phase where the \mathbb{Z}_2 parity symmetry of the total number of excitations \hat{N} is spontaneously broken. Finally, for $g > g_c$ and $E_k(g) > E_c$, the symmetry is restored and the model is again in the normal phase. The excited-state QPT takes place at the critical energy $E_c = -\Omega/2$ [52]. Besides the microscopic details, the universal critical features are equivalent to those of the LMG model, with a similar energy spectrum as the one depicted in Fig. 1 (note however the difference in the location of the normal ($g < g_c$) and symmetry-breaking phases ($g > g_c$)).

In the following, we exemplify that the AQIS also applies to the QRM. For that, we choose

$$|\psi_0\rangle = |\alpha\rangle_m |0\rangle_s, \quad (19)$$

as our initial symmetry-breaking state. There $|\alpha\rangle_m = \hat{D}(\alpha) |0\rangle_m = \exp[\alpha \hat{a}^\dagger - \alpha^* \hat{a}] |0\rangle_m$ represents a coherent state with amplitude α and $|0\rangle_m$ the vacuum state, while the spin is its ground

state, $\hat{\sigma}_z |0\rangle_s = -|0\rangle_s$. This corresponds to a state in other of the wells of the effective double-well potential in the symmetry-breaking phase [51, 52]. The symmetry-breaking information is then attributed to the expectation value of the position operator $\hat{x} = (\hat{a}^\dagger + \hat{a})/\sqrt{2}$.

The adiabatic protocol is performed from $g_0 = 2$ to g_1 , according to Eq. (5). Relying on the adiabatic approximation and choosing $\alpha = 5$ for a critical QRM with $\Omega = 100\omega$, we compute the final state and obtain $\langle\psi(2\tau)|\hat{x}|\psi(2\tau)\rangle$ as a function of g_1 . Numerical simulations have been performed with 1000 Fock states. The results are gathered in Fig. 7. First, the energy probability distribution is shown in Fig. 7(a), indicating that the state is contained within the symmetry-breaking phase since all the populated eigenstates have energies below the critical one $E_c = -\Omega/2$. As before, the AQIS becomes effective when the whole state is driven into the normal phase. For the considered initial state, this happens for $g_1 \lesssim 1.5$ (cf. Fig. 7(b) and (c)). Note that this corresponds to a larger parameter than its critical value $g_c = 1$ where the QPT takes place. Instead, the value $g \approx 1.5$ marks the position when the energy of the adiabatically-driven state surpasses the critical energy at which an excited-state QPT occurs [52].

5 Conclusions

In this article, we have analyzed the adiabatic scrambling of the symmetry-breaking information encoded in an initial state. The mechanism for such adiabatic quantum information scrambling is detailed, which is related to the difference of accumulated phases among degenerated eigenstates due to the driving from a symmetry-breaking into a normal phase, and thus to phase transitions taking place both in the ground and excited states of the system. Owing to its adiabatic nature, the protocol does not alter either the energy or the expectation values of observables independent of the symmetry-breaking information. To the contrary, as a consequence of the scrambling, the expectation value of an operator that quantifies the symmetry-breaking becomes approximately zero provided the initial state has a large support in the eigenstates of the Hamiltonian and the relative difference among the accumulated phases of eigenstates of opposite parity are uniformly distributed. We showcase the adiabatic quantum information scrambling in the Lipkin-Meshkov-Glick and quantum Rabi models and quantify the effectiveness of the scrambling for different initial states. The potential information retrieval is studied utilizing the Loschmidt echo, which indicates that an effective scrambling would require an almost perfect time-reversal protocol to restore the initial information. Our results demonstrate the intriguing interplay between quantum information, many-body systems, and critical phenomena.

Acknowledgments

F.J.G- R is grateful for financial support from the Spanish MCIN with funding from the European Union Next Generation EU (PRTRC17.I1) and the Consejería de Educación from Junta de Castilla y Leon through the QCAYLE project, as well as grants PID2020-113406GB-I00 MTM funded by AEI/10.13039/501100011033, and RED2022-134301-T

References

- [1] B. Swingle, G. Bentsen, M. Schleier-Smith, and P. Hayden, *Phys. Rev. A* **94**, 040302 (2016).

- [2] B. Swingle, *Nat. Phys.* **14**, 988 (2018).
- [3] S. Xu and B. Swingle, *PRX Quantum* **5**, 010201 (2024).
- [4] J. M. Deutsch, *Phys. Rev. A* **43**, 2046 (1991).
- [5] A. Touil and S. Deffner, *PRX Quantum* **2**, 010306 (2021).
- [6] A. Touil and S. Deffner, *Europhysics Letters* **146**, 48001 (2024).
- [7] M. A. Nielsen and I. L. Chuang, *Quantum computation and quantum information* (Cambridge University Press, Cambridge, England, 2000).
- [8] M. Mezei and D. Stanford, *J. High Energy Phys.* **2017** (2017).
- [9] A. Chenu, J. Molina-Vilaplana, and A. del Campo, *Quantum* **3**, 127 (2019).
- [10] M. Campisi and J. Goold, *Physical Review E* **95** (2017), 10.1103/physreve.95.062127.
- [11] S. Deffner and S. Campbell, *Quantum Thermodynamics*, 2053-2571 (Morgan & Claypool Publishers, 2019).
- [12] J. Maldacena, S. H. Shenker, and D. Stanford, *Journal of High Energy Physics* **2016** (2016), 10.1007/jhep08(2016)106.
- [13] A. Polkovnikov, K. Sengupta, A. Silva, and M. Vengalattore, *Rev. Mod. Phys.* **83**, 863 (2011).
- [14] J. Eisert, M. Friesdorf, and C. Gogolin, *Nature Physics* **11**, 124 (2015).
- [15] S. Sachdev, *Quantum phase transitions*, 2nd ed. (Cambridge University Press, Cambridge, UK, 2011).
- [16] M. Srednicki, *Phys. Rev. E* **50**, 888 (1994).
- [17] A. M. Kaufman, M. E. Tai, A. Lukin, M. Rispoli, R. Schittko, P. M. Preiss, and M. Greiner, *Science* **353**, 794 (2016).
- [18] M. Rigol, V. Dunjko, and M. Olshanii, *Nature* **452**, 854 (2008).
- [19] X. Mi, P. Roushan, C. Quintana, and *et al.*, *Science* **374**, 1479 (2021).
- [20] Q. Zhu, Z.-H. Sun, M. Gong, F. Chen, Y.-R. Zhang, Y. Wu, Y. Ye, C. Zha, S. Li, S. Guo, H. Qian, H.-L. Huang, J. Yu, H. Deng, H. Rong, J. Lin, Y. Xu, L. Sun, C. Guo, N. Li, F. Liang, C.-Z. Peng, H. Fan, X. Zhu, and J.-W. Pan, *Phys. Rev. Lett.* **128**, 160502 (2022).
- [21] F. J. Gómez-Ruiz, J. J. Mendoza-Arenas, F. J. Rodríguez, C. Tejedor, and L. Quiroga, *Physical Review B* **97** (2018), 10.1103/physrevb.97.235134.
- [22] K. A. Landsman, C. Figgatt, T. Schuster, N. M. Linke, B. Yoshida, N. Y. Yao, and C. Monroe, *Nature* **567**, 61 (2019).
- [23] M. Gärttner, J. G. Bohnet, A. Safavi-Naini, M. L. Wall, J. J. Bollinger, and A. M. Rey, *Nature Physics* **13**, 781 (2017).
- [24] Y.-L. Zhang, Y. Huang, and X. Chen, *Phys. Rev. B* **99**, 014303 (2019).

- [25] Y. Huang, F. G. S. L. Brandão, and Y.-L. Zhang, *Phys. Rev. Lett.* **123**, 010601 (2019).
- [26] V. Alba and P. Calabrese, *Phys. Rev. B* **100**, 115150 (2019).
- [27] J.-H. Wang, T.-Q. Cai, X.-Y. Han, Y.-W. Ma, Z.-L. Wang, Z.-H. Bao, Y. Li, H.-Y. Wang, H.-Y. Zhang, L.-Y. Sun, Y.-K. Wu, Y.-P. Song, and L.-M. Duan, *Phys. Rev. Res.* **4**, 043141 (2022).
- [28] S. Omanakuttan, K. Chinni, P. D. Blocher, and P. M. Poggi, *Phys. Rev. A* **107**, 032418 (2023).
- [29] P. Cejnar, M. Macek, S. Heinze, J. Jolie, and J. Dobeš, *J. Phys. A: Math. Theor.* **39**, L515 (2006).
- [30] M. Caprio, P. Cejnar, and F. Iachello, *Ann. Phys. (N. Y.)* **323**, 1106 (2008).
- [31] T. Brandes, *Phys. Rev. E* **88**, 032133 (2013).
- [32] P. Stránský, M. Macek, and P. Cejnar, *Ann. Phys. (N. Y.)* **345**, 73 (2014).
- [33] P. Stránský, M. Macek, A. Leviatan, and P. Cejnar, *Ann. Phys. (N. Y.)* **356**, 57 (2015).
- [34] P. Cejnar, P. Stránský, M. Macek, and M. Kloc, *Journal of Physics A: Mathematical and Theoretical* **54**, 133001 (2021).
- [35] R. Puebla, A. Relaño, and J. Retamosa, *Phys. Rev. A* **87**, 023819 (2013).
- [36] R. Puebla and A. Relaño, *Europhys. Lett.* **104**, 50007 (2013).
- [37] R. Puebla and A. Relaño, *Phys. Rev. E* **92**, 012101 (2015).
- [38] A. L. Corps and A. Relaño, *Phys. Rev. Lett.* **127**, 130602 (2021).
- [39] A. L. Corps and A. Relaño, *Phys. Rev. B* **106**, 024311 (2022).
- [40] A. L. Corps and A. Relaño, *Phys. Rev. Lett.* **130**, 100402 (2023).
- [41] F. J. Gómez-Ruiz, O. L. Acevedo, F. J. Rodríguez, L. Quiroga, and N. F. Johnson, *Frontiers in Physics* **6** (2018), 10.3389/fphy.2018.00092.
- [42] F. Gómez-Ruiz, O. Acevedo, L. Quiroga, F. Rodríguez, and N. Johnson, *Entropy* **18**, 319 (2016).
- [43] H. Lipkin, N. Meshkov, and A. Glick, *Nucl. Phys.* **62**, 188 (1965).
- [44] S. Dusuel and J. Vidal, *Phys. Rev. Lett.* **93**, 237204 (2004).
- [45] F. Leyvraz and W. D. Heiss, *Phys. Rev. Lett.* **95**, 050402 (2005).
- [46] J. Vidal, S. Dusuel, and T. Barthel, *J. Stat. Mech.* **2007**, P01015 (2007).
- [47] P. Ribeiro, J. Vidal, and R. Mosseri, *Phys. Rev. Lett.* **99**, 050402 (2007).
- [48] P. Ribeiro, J. Vidal, and R. Mosseri, *Phys. Rev. E* **78**, 021106 (2008).

- [49] R. H. Dicke, [Phys. Rev. **93**, 99 \(1954\)](#).
- [50] C. Emary and T. Brandes, [Phys. Rev. Lett. **90**, 044101 \(2003\)](#).
- [51] M.-J. Hwang, R. Puebla, and M. B. Plenio, [Phys. Rev. Lett. **115**, 180404 \(2015\)](#).
- [52] R. Puebla, M.-J. Hwang, and M. B. Plenio, [Phys. Rev. A **94**, 023835 \(2016\)](#).
- [53] L. Bakemeier, A. Alvermann, and H. Fehske, [Phys. Rev. A **85**, 043821 \(2012\)](#).
- [54] R. Puebla, [Phys. Rev. B **102**, 220302 \(2020\)](#).
- [55] S. Felicetti and A. Le Boité, [Phys. Rev. Lett. **124**, 040404 \(2020\)](#).
- [56] M. A. Bastarrachea-Magnani, S. Lerma-Hernández, and J. G. Hirsch, [Phys. Rev. A **89**, 032102 \(2014\)](#).
- [57] A. Relaño, M. A. Bastarrachea-Magnani, and S. Lerma-Hernández, [Europhysics Letters **116**, 50005 \(2017\)](#).
- [58] C. M. Lóbez and A. Relaño, [Phys. Rev. E **94**, 012140 \(2016\)](#).
- [59] Ángel L Corps, R. A. Molina, and A. Relaño, [Journal of Physics A: Mathematical and Theoretical **55**, 084001 \(2022\)](#).
- [60] T. Zibold, E. Nicklas, C. Gross, and M. K. Oberthaler, [Phys. Rev. Lett. **105**, 204101 \(2010\)](#).
- [61] P. Jurcevic, H. Shen, P. Hauke, C. Maier, T. Brydges, C. Hempel, B. P. Lanyon, M. Heyl, R. Blatt, and C. F. Roos, [Phys. Rev. Lett. **119**, 080501 \(2017\)](#).
- [62] T. Caneva, R. Fazio, and G. E. Santoro, [Phys. Rev. B **78**, 104426 \(2008\)](#).
- [63] H.-M. Kwok, W.-Q. Ning, S.-J. Gu, and H.-Q. Lin, [Phys. Rev. E **78**, 032103 \(2008\)](#).
- [64] Z.-G. Yuan, P. Zhang, S.-S. Li, J. Jing, and L.-B. Kong, [Phys. Rev. A **85**, 044102 \(2012\)](#).
- [65] O. L. Acevedo, L. Quiroga, F. J. Rodríguez, and N. F. Johnson, [Phys. Rev. Lett. **112**, 030403 \(2014\)](#).
- [66] G. Salvatori, A. Mandarino, and M. G. A. Paris, [Phys. Rev. A **90**, 022111 \(2014\)](#).
- [67] S. Campbell, G. De Chiara, M. Paternostro, G. M. Palma, and R. Fazio, [Phys. Rev. Lett. **114**, 177206 \(2015\)](#).
- [68] S. Campbell, [Phys. Rev. B **94**, 184403 \(2016\)](#).
- [69] N. Defenu, T. Enss, M. Kastner, and G. Morigi, [Phys. Rev. Lett. **121**, 240403 \(2018\)](#).
- [70] R. Puebla, A. Smirne, S. F. Huelga, and M. B. Plenio, [Phys. Rev. Lett. **124**, 230602 \(2020\)](#).
- [71] Z. Mzaouali, R. Puebla, J. Goold, M. El Baz, and S. Campbell, [Phys. Rev. E **103**, 032145 \(2021\)](#).
- [72] L. Garbe, O. Abah, S. Felicetti, and R. Puebla, [Quantum Science and Technology **7**, 035010 \(2022\)](#).

- [73] J. Gamito, J. Khalouf-Rivera, J. M. Arias, P. Pérez-Fernández, and F. Pérez-Bernal, [Phys. Rev. E **106**, 044125 \(2022\)](#).
- [74] L. Garbe, O. Abah, S. Felicetti, and R. Puebla, [Phys. Rev. Res. **4**, 043061 \(2022\)](#).
- [75] O. Abah, G. De Chiara, M. Paternostro, and R. Puebla, [Phys. Rev. Res. **4**, L022017 \(2022\)](#).
- [76] A. Santini, L. Lumia, M. Collura, and G. Giachetti, [arXiv:2407.20314 \(2024\)](#).
- [77] P. Cejnar and P. Stránský, [Phys. Rev. E **78**, 031130 \(2008\)](#).
- [78] P. Pérez-Fernández and A. Relaño, [Phys. Rev. E **96**, 012121 \(2017\)](#)